

INTEGRATION OF TERRESTRIAL AND AIRBORNE LIDAR DATA FOR SYSTEM CALIBRATION

Ki In Bang^{a,*}, Ayman F. Habib^a, Kresimir Kusevic^b, Paul Mrstik^b

^a Department of Geomatics Engineering, University of Calgary, Canada - (habib, kibang)@ucalgary.ca

^b Terrapoint Inc., Canada - (kresimir.kusevic, paul.mrstik)@terrapoint.com

Commission I, WG I/2

KEY WORDS: LiDAR, Calibration, Quality Assurance, System Biases, Areal Features, Surface Matching

ABSTRACT:

The ever improving capabilities of the direct geo-referencing technology is having a positive impact on the widespread adoption of LiDAR systems for the acquisition of dense and accurate surface models over extended areas. LiDAR systems can quickly provide accurate surface models with a dense set of irregular points, surpassing the quality of those derived from other techniques, such as manual photogrammetric DSM generation, radar interferometry, and contour interpolation. A typical LiDAR system consists of three main components: a GNSS to provide position information, an INS for attitude determination, and a laser scanner to provide the range/distance from the laser-beam firing point to its footprint. The accuracy of the LiDAR point cloud is ensured by the quality of the measurements from the individual system components and their spatial relationship as defined by the bore-sighting parameters. Even though the measurements of the individual system components (GNSS, INS and laser scanner) are quite precise, serious errors can result from inaccurate estimation of the bore-sighting parameters. For this reason, bore-sighting parameters should be well defined at the beginning of the work process and will be the focus of this paper. This paper presents a new methodology for simultaneous estimation of the LiDAR bore-sighting parameters using control features that are automatically extracted from a reference control surface. In this approach, the reference control surface is derived from a terrestrial LiDAR system. The shorter ranges and the high point density associated with terrestrial LiDAR systems would ensure the generation of a reference surface, which is accurate enough for reliable estimation of the calibration parameters associated with airborne LiDAR systems. After introducing the mathematical models for the proposed methodologies, this paper outlines the optimal configuration of the control data for a reliable estimation of the calibration parameters, while avoiding possible correlations among these parameters. Finally, the feasibility test presents experimental results from real datasets while highlighting the advantages and the limitations of the proposed methodologies.

1. INTRODUCTION

1.1 Basics of a LiDAR System

Recently, LiDAR systems have been proven as a cost-effective tool for the generation of surface models over extended areas. They can quickly provide accurate surface models with a dense set of irregular points, surpassing the quality of those derived from other techniques, such as manual photogrammetric DSM generation, radar interferometry, and contour interpolation. A typical LiDAR system consists of three main components, a GNSS system to provide position information, an INS unit for attitude determination, and a laser system to provide range (distance) information between the laser firing point and the ground point. In addition to range data, modern LiDAR systems can capture intensity images over the mapped area. Therefore, LiDAR is being more extensively used in mapping and GIS applications.

Figure 1 shows a schematic diagram of a LiDAR system together with the involved coordinate systems. Equation 1 is the basic LiDAR geometric model that incorporates the LiDAR measurements for deriving positional information. This equation relates four coordinate systems, which include the ground coordinate system, the inertial measurement unit (IMU)

body frame coordinate system, the laser unit coordinate system, and the laser beam coordinate system. This equation is simply the result of a three vector summation; \vec{X}_0 is the vector from the origin of the ground coordinate system to the IMU body frame, \vec{P} is the offset between the laser unit and the GNSS phase center with respect to IMU body frame, and $\vec{\rho}$ is the vector between the laser beam firing point and the object point, which is defined in the laser beam frame. The summation of these three vectors after applying the appropriate rotations ($R_{INS}, R_{\Delta}, R_{scan}$) will yield the vector \vec{X} , which represents the ground coordinates of the object point under consideration. The quality of the derived surface depends on the accuracy of the involved sub-systems (i.e., laser, GNSS, and INS) and the calibration parameters relating these components (i.e., bore-sighting parameters).

Even though the individual measurement capabilities of the system components (GNSS, INS and laser scanner system) are quite precise, serious errors can occur from inaccurate combination of these components. For this reason, bore-sighting parameters should be well calibrated before surveying missions. The ultimate goal of the LiDAR system calibration is to determine all systematic parameters involved in a LiDAR equation and to obtain the correct raw measurements. The

* Corresponding author

LiDAR system calibration is done through several procedures. In the first step, individual sensors are calibrated in the laboratory. After that, mounting parameters are determined after installing sensors on a platform. In the last step, in-situ calibrations are done before and after surveying missions (Schenk 2001).

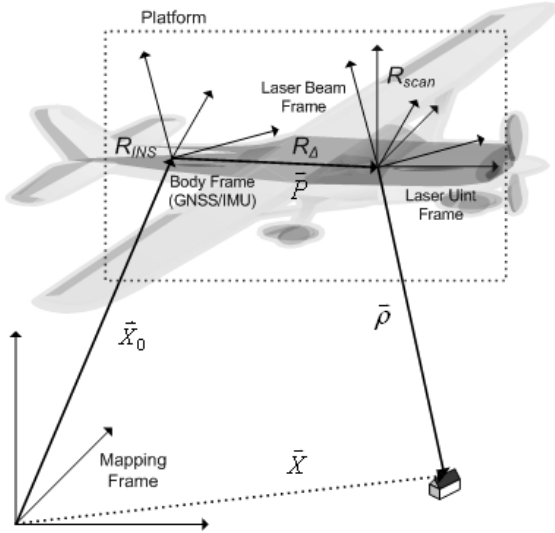


Figure 1. Coordinates and parameters involved in a LiDAR acquisition system

$$\bar{X} = \bar{X}_0 + R_{\omega\phi\kappa} \bar{P} + R_{\omega\phi\kappa} R_{\Delta\omega\Delta\phi\Delta\kappa} R_{\beta} \begin{bmatrix} 0 \\ 0 \\ -\rho \end{bmatrix} \quad (1)$$

1.2 Previous Researches

In the past few years, several research methods for LiDAR calibration have been developed. For example, Schenk (2001) investigated the sources of systematic errors that can occur in a LiDAR system. A calibration procedure was then proposed using such an analysis. This work revealed that some of the calibration parameters cannot be easily estimated due to their strong correlation. The calibration methodology developed by Morin (2002) uses the LiDAR equation to solve for the bore-sighting misalignment angles and the scanner angle correction. These parameters are either estimated using ground control points or by observing discrepancies between tie points in overlapping strips. However, the identification of distinct control and tie points in LiDAR data is a difficult task due to the irregular nature of the collected point cloud. To alleviate this difficulty, Skaloud and Lichti (2006) presented a calibration technique using tie planar patches in overlapping strips. The underlying assumption of this procedure is that systematic errors in the LiDAR system will lead to non-coplanarity of conjugate planar patches as well as bending effects in these patches. The calibration process uses the LiDAR equation to simultaneously solve for the plane parameters as well as the bore-sighting misalignment angles. However, this approach requires having large planar patches, which might not always be available. In addition, systematic biases, which would not affect the coplanarity of conjugate planar patches, could still remain. The approaches taken by

LiDAR surveying companies were more closely applicable in practice. For example, to calibrate the LiDAR system, Hanjin (2006) devised a calibration field which is composed of well-known surfaces. Using the calibration site, discrepancies between the LiDAR point cloud and the reference surface are observed and used to determine the system parameters such as the bore-sighting roll and pitch angles and scale parameters. The drawbacks of this approach are that the method involves manual and empirical procedures, and some parameters are not considered in the calibration procedure.

This paper presents a new methodology for simultaneous estimation of the LiDAR bore-sighting parameters using control features that are automatically extracted from a reference control surface. In this approach, the reference control surface is derived from a terrestrial LiDAR system. The shorter ranges and the high point density associated with terrestrial LiDAR systems would ensure the generation of a reference surface, which is accurate enough for reliable estimation of the calibration parameters associated with airborne LiDAR systems.

2. PROPOSED METHODS

2.1 Point Primitives and ICP method

The main issue considered in the proposed calibration procedure is identifying conjugate features in the airborne and terrestrial LiDAR systems. As mentioned above, due to the irregular nature of the generated point cloud from a LiDAR system, it is usually believed that there is no point-to-point correspondence between the derived points from the airborne and terrestrial systems. However, one might argue that point-to-point correspondences for a fraction of the terrestrial and airborne datasets can be assumed; considering the higher point density associated with terrestrial systems compared with that for airborne systems and the noise level in both datasets.

Therefore, this paper introduces a point-based calibration procedure using pseudo-conjugate points in the terrestrial and airborne datasets, and Equation 2 shows the target function based on the point primitives for the calibration. In this Equation, the superscription T denotes the target data (airborne LiDAR data), while R denotes the reference data (Point cloud generated by terrestrial LiDAR system). While only point cloud coordinates are utilized from the reference data, LiDAR system raw measurements should be available for the target system. As shown in

Figure 2, two points are used from both datasets, and

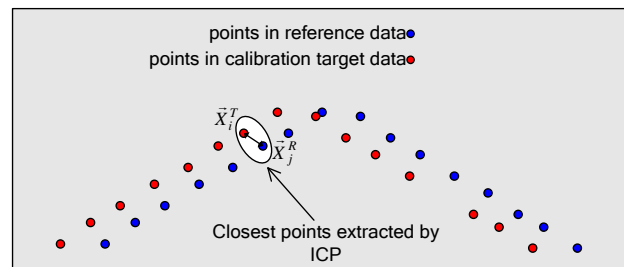


Figure 2. The closest points selected by the iterative closest point procedure

those points are selected by the iterative closest point (ICP) procedure (Zhang, 1994), which is one of the common surface matching method. After that, in the calibration procedure, two

corresponding points are considered as pseudo-conjugate points, and the best estimated calibration parameters are obtained when the distance between two points are minimized.

Figure 4 shows that the ICP procedure is used to sequentially identify pseudo-conjugate points in the datasets, which are then used to estimate the calibration parameters for the airborne system. The iterative procedure will continue until there are no significant changes in the estimated parameters.

$$\bar{X}_j^R = \bar{X}_i^T \begin{pmatrix} \bar{X}_{0_i} + R_{\omega\phi\kappa_i} \bar{P} + R_{\omega\phi\kappa_i} R_{\Delta\omega\Delta\phi\Delta\kappa} R_{\beta_i} \begin{bmatrix} 0 \\ 0 \\ -\rho_i \end{bmatrix} \end{pmatrix} \quad (2)$$

2.2 Point/Patch Primitives and ICPatch method

For instances where no point-to-point correspondence between the terrestrial and airborne datasets can be assumed, one should consider alternative primitives for the calibration procedure. Instead of distinct points, one can use areal features, which can be identified in both data: calibration data and reference data. Such primitives, however, would require pre-processing of the LiDAR point cloud to extract areal features (e.g., segmentation, and plane fitting). In this research, we aim at selecting primitives, which can be derived with minimal pre-processing of the original LiDAR footprints. Moreover, the selected primitives should be reliably derived in any type of environment (e.g., urban and rural areas). To satisfy these objectives, we chose to represent airborne LiDAR data using the original footprints, while terrestrial LiDAR data is represented by triangular patches, which can be derived from a Triangulated Irregular Network (TIN) generation procedure. Figure 3 illustrates the case where the airborne LiDAR data denoted by \bar{X}^T is represented by a set of points while the terrestrial LiDAR denoted by \bar{X}^R is represented by a set of triangular patches. Due to the high density of the terrestrial LiDAR data as well as the relatively smooth characteristics of terrain and man-made structures, using TIN patches to describe the physical surface is quite acceptable. Corresponding point-to-patch is extracted by the iterative closest patch (ICPatch) procedure from TIN and irregular point data (Habib, 2006). After that, in the calibration procedure, the selected corresponding point and

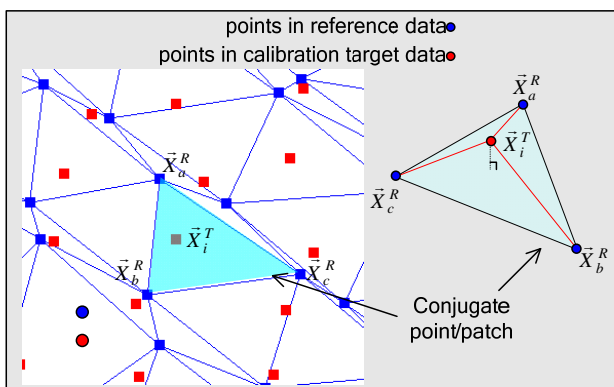


Figure 3. The closest patch and point selected by the iterative closest patch procedure

patch are used as alternative primitives, and the adapted constraints for the calibration is the determinant of the four points: three points of the triangular patch and the point of irregular point data. Equation 3 shows the mathematical form of the determinant of four points; where \bar{X}_a^R , \bar{X}_b^R , and \bar{X}_c^R are vertices of triangular patch, and \bar{X}_i^T denotes the corresponding point from the airborne LiDAR data. The best estimated calibration parameters are obtained when the determinants are minimized.

Figure 4 shows that the ICPatch method is used to sequentially identify conjugate point/patch pairs in the both datasets, and the recursive adjustment procedure will continue until there are no significant changes in the estimated calibration parameters.

$$\det \begin{bmatrix} X_i^T & Y_i^T & Z_i^T & 1 \\ X_a^R & Y_a^R & Z_a^R & 1 \\ X_b^R & Y_b^R & Z_b^R & 1 \\ X_c^R & Y_c^R & Z_c^R & 1 \end{bmatrix} = 0 \quad (3)$$

$$\bar{X}_i^T = f(obs_i^T, P)$$

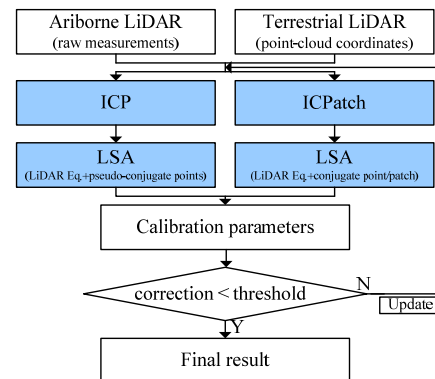


Figure 4. The calibration procedure using ICP and ICPatch methods

2.3 Planar Patches and Modified Weight Matrix

In this paper, the plane segmentation for the areal patches is introduced as an alternative approach that utilizes conjugate planar patches for the calibration procedure. The patches are extracted through an automated segmentation procedure. Then the conjugate patches are identified through checking their overlap, the compatibility of their surface normals, and their spatial distance. The matched planar patches are used in a point-based calibration procedure, which is similar to the approach using the point primitive and ICP procedure. In general, conjugate planar patches used with an additional constraint such as the normal distance, but this proposed approach uses pseudo-conjugate points and modified weight matrices instead of additional constraints.

Figure 5 shows two planar patches which are extracted from terrestrial LiDAR data (reference data) and airborne LiDAR data (target data) respectively. The point \bar{X}^R and \bar{X}^T are not exactly conjugate points, but both points belong to the same object plane. To compensate for the fact that non-conjugate points are used based on the point primitive, the error ellipse is

expanded along the plane, and the modified weight matrices are calculated by the orientation of the plane and the expanded error ellipse. In Equation 4, Σ'_{UVW} is the modified variance-covariance matrix of the selected point on the plane, and the relationship between XYZ and UVW spaces is explained by the rotation matrix R , which is derived from plane equation parameters. As shown in Figure 5, the direction of W axis is parallel to the normal vector of the plane, and M_U and M_V are applied to the variance-covariance matrix to expand the error ellipse along the plane. At last, the modified weight matrix P' is derived using the R and Σ'_{UVW} matrices as shown in Equation

4. The system calibration parameters are obtained by a least square adjustment procedure with the modified weight matrix. This approach is sequentially described using the flow chart in Figure 6. The main advantage of this procedure is having a single algorithm for simultaneously handling conjugate points and planar patches, if available. The limitation of this approach is its dependency on the presence of planar patches in the available data.

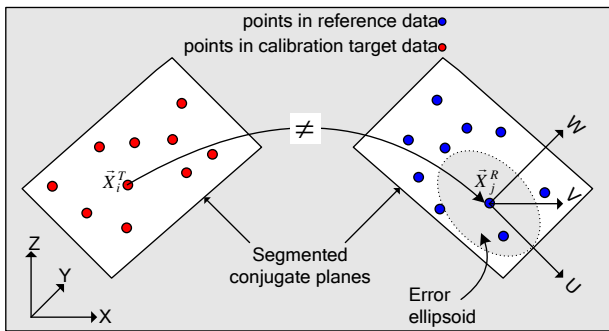


Figure 5. Conjugate planar patches and expanded error ellipse

$$P' = (\Sigma'_{XYZ})^{-1} = (R^T \Sigma'_{UVW} R)^{-1}$$

$$\Sigma'_{UVW} = \begin{bmatrix} \sigma_U^2 + M_U & \sigma_{UV} & \sigma_{UW} \\ \sigma_{VU} & \sigma_V^2 + M_V & \sigma_{VW} \\ \sigma_{WU} & \sigma_{WV} & \sigma_W^2 \end{bmatrix} \quad (4)$$

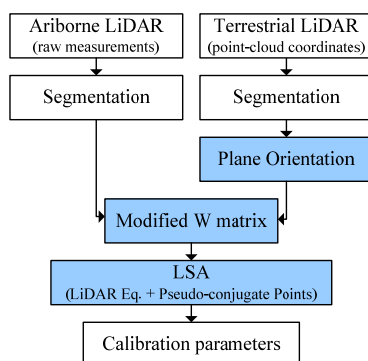


Figure 6. The calibration procedure using planar patches and modified weight matrices

To ensure a reliable estimation of the system parameters, the utilized planar patches must represent sloping surfaces with different aspects (i.e., to avoid possible correlation among

parameters). The next section outlines the optimal configuration of the control patches for a reliable estimation of the calibration parameters, while avoiding possible correlations among these parameters.

2.4 Optimum Configuration of Planar Patches

When using planar patches as alternative primitives, one should give attention to the optimum configuration of planar patches because that condition is the one that yields an accurate estimate of the parameters while avoiding any possible correlations among them. In general, we do not expect that significant errors exist in the directly measured spatial offsets between the GNSS/INS and laser scanner of a LiDAR system. However, if we can de-couple the spatial and rotational offsets relating these components, we can simultaneously estimate the angular and spatial bore-sighting parameters. For the control patches, the ideal configuration is shown in Figure 7.a, which illustrates orthogonal patches in the XY , XZ , and YZ planes. Unfortunately this situation is not realistic (i.e., it is not always guaranteed that such a configuration is available in a LiDAR data captured from an airborne system).

A more realistic planar patch configuration is shown in Figure 7.b. For this configuration, horizontal and sloping planar patches are used for the calibration process. It is important to have sloping planar patches with different aspects (e.g., some of the patches can be parallel to the X -axis while others are parallel to the Y -axis).

To test the performance of this configuration together with the impact of the slope of such patches, we simulated a LiDAR strip using a linear scanner system at 1,500 m flying height with 25 degree scan angle. The simulation process started with a surface model and system trajectory. Using such information, we produced synthetic LiDAR data including system raw measurement such as GNSS, INS, and laser scanner measurements, which were then used to estimate the bore-sighting parameters. After preparing simulated LiDAR data, the discrepancies were analyzed to compare the original and reconstructed surfaces using system parameters and raw measurements.

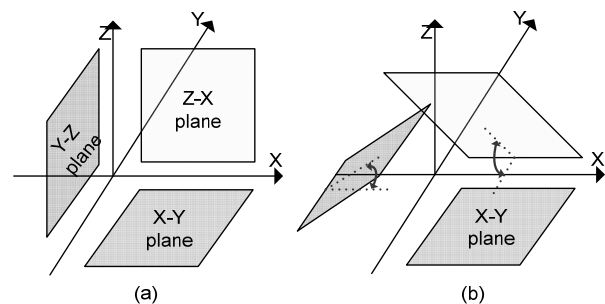


Figure 7. Optimal (a) and realistic (b) planar patches for the LiDAR system calibration

Figure 8 shows the accuracy of the reconstructed coordinates using the recovered bore-sighting parameters from well-distributed 5 control patches along the LiDAR swath with varying slopes.

Figure 9 shows the discrepancies between the true bore-sighting parameters and recovered ones. As it can be seen in these two figures, if the slope of the planes is very small (e.g., less than 10 degree), the planar patches are almost parallel, and the RMSE of the reconstructed coordinates of LiDAR points are very high. It is also seen that for such a case, the derived bore-sighting parameters are not close to the true parameters. Therefore, it is recommended that some of the control patches should have slopes that exceed 10 degrees. Moreover, the patches should have different orientation in space (i.e., different aspect angles).

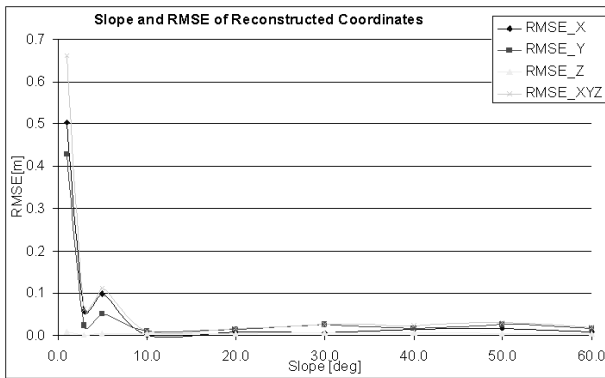


Figure 8. Slope of planar patches and accuracies of reconstructed surface

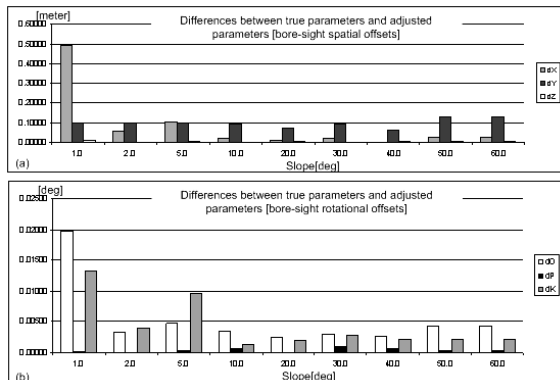


Figure 9. Differences between the true and estimated bore-sighting parameters

3. EXPERIMENTS

In the first test, virtual LiDAR data was simulated and used to confirm the feasibility of the proposed methods. For the test data, airborne and terrestrial LiDAR systems are considered in an urban area. The airborne system flew over the area at around 90m flying height, and the terrestrial system mainly scanned building walls along the road. As shown in

Figure 10, the terrestrial data consists of two strips, which are left and right sides of the road.

The results from the simulation data are shown in Table 1. As a result, the re-covered calibration parameters are very close to the expected values in all of methods, and these results are good enough to confirm the feasibility of the proposed calibration methodologies in this paper. The differences between

parameters recovered using different three approaches are very small, and it can be ignored. The simulation data is relatively ideal compared to the real data. Anyway, the ultimate goal of the calibration test using simulation data is to confirm the feasibility of the methods and detect any possible drawbacks.

The next, the author introduces the experiment results from real airborne and terrestrial LiDAR data. The results are relatively worse than the simulation test, because the quality of this real data is not guaranteed. Especially, the terrestrial data has some drift errors in INS navigation data; there was, however, no available other terrestrial LiDAR data.

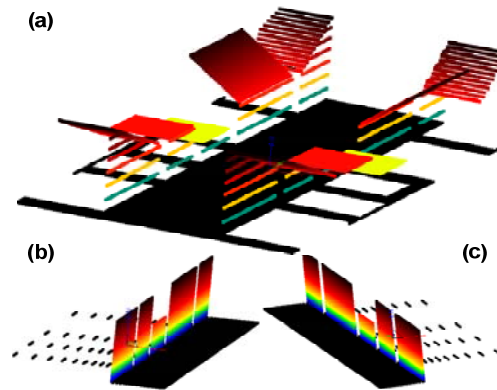


Figure 10. Simulated LiDAR data: (a) is airborne LiDAR data, and (b)&(c) are terrestrial LiDAR data.

	ΔX (m)	ΔY (m)	ΔZ (m)	$\Delta \omega$ (deg)	$\Delta \phi$ (deg)	$\Delta \kappa$ (deg)
True Parameters	0.1	0.1	0.1	1.0	1.0	1.0
ICP	0.11	0.98	0.10	1.00	1.00	1.00
	Norm[m] : 0.050			σ : 0.063		
ICPatch	0.09	0.10	0.09	1.01	1.02	0.98
	Norm[m] : 0.054			σ : 0.071		
Planar Patches	0.11	0.10	0.10	1.00	1.00	1.00
	Norm[m] : 0.035			σ : 0.051		

Table 1. The LiDAR system calibration test using simulation data (6 bore-sighting parameters)

Table 2 shows the description of used data; the point density of the terrestrial LiDAR data is about 2.7 times that of the airborne LiDAR data. The airborne data was captured at a 150m flying height from the ground-level, while the average range of the terrestrial data is less than 20m.

	Reference Data	Target Data
System Def-ID	Titan Laser 1	Plate# 3
Point density	13.5 points/m ²	5 points/ m ²
System Def-Time	1-Mar, 2007	11-Nov, 2006
Flying height	N/A	150m

Table 2. Description about test LiDAR data

Figure 11 shows the used real data figures; (a) represents the terrestrial LiDAR data used as the reference surface, and (b)

represents the airborne LiDAR data. Terrestrial data covers very narrow areas compared to the airborne data, but the point density is much higher. Even though small areas are selected from the terrestrial data for the process, the process can take some time, and one should give attention to the lack of a computer memory for computation. Both data were captured in the same area, but the overlap area of the two systems is not large.

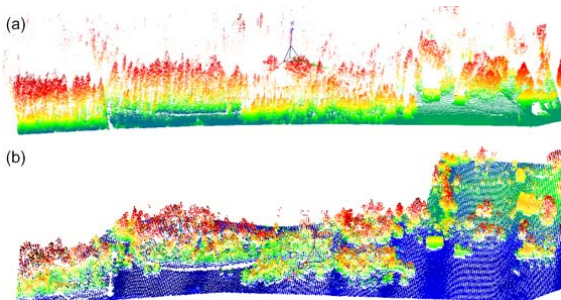


Figure 11. Terrestrial laser scanning data (a) is used as reference data to calibrate airborne laser scanning data (b)

	ΔX (m)	ΔY (m)	ΔZ (m)	$\Delta \omega$ (deg)	$\Delta \phi$ (deg)	$\Delta \kappa$ (deg)
Given parameters	0.210	0.190	-0.003	0.168	-0.035	0.000
	Norm[m] : 0.159			N/A		
ICP	-0.163	-0.080	-0.087	0.068	-0.052	0.118
	Norm[m] : 0.119			σ : 0.113		
ICPatch	-0.032	-0.015	0.026	0.009	-0.012	0.018
	Norm[m] : 0.139			σ : 0.125		
Planar Patches	0.108	-0.495	-0.003	0.174	0.040	-0.032
	Norm[m] : 0.129			σ : 0.120		

Table 3. The LiDAR system calibration test using real data (6 bore-sighting parameters)

Table 3 shows the adjusted bore-sighting parameters from the proposed methods, respectively. To evaluate the adjusted parameters, average normal distances between the adjusted surface and reference surface are calculated. After the object surfaces are re-constructed using the new system parameters, a surface matching procedure was then carried out to find corresponding points between both data; ICPatch was used for this purpose, in this case. Consequently, normal distances between matched points and triangular patches are calculated. The real LiDAR data was captured along the rail-road areas in eastern Canada, and these areas are quite rural. Hence, it was hard to extract the planar patches, especially from man-made objects such as buildings. Since the distribution and configuration of control patches are important in terms of possible correlations between calibration parameters, one should give attention to the extraction of control data. From the control feature selection point of view, the other two approaches, using ICP and ICPatch, appear easier and more effective. These two methods, however, are very sensitive to the initial approximations and random error size. Even though pseudo-conjugate points from the ICP procedure and triangular patches from TIN are easier approaches in terms of establishing corresponding points for the rural areas, like this test area, the method using segmented planar patches can have reliable solutions and is not sensitive to the ill conditioned data like high random errors, if planar patches can satisfy the required

condition; configuration and distribution. For these reasons, large and abundant planar patches are relatively better than the closest points and the closest TIN element; which are not very sensitive to random errors and initial approximations. Furthermore artificial control planar targets and well-known man-made objects can be considered as the ideal control data for the system calibration.

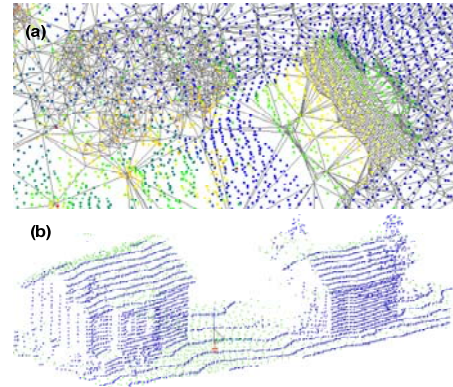


Figure 12. (a) the TIN represents the reference data and points denote target data in 2D display. (b) in 3D display, reference data (terrestrial LiDAR) is mainly appeared along the vertical wall, while the points of the target data (airborne LiDAR) are very dense on the ground.

4. CONCLUSIONS

In this paper, the author introduces the airborne LiDAR system calibration procedure using the terrestrial LiDAR data which is capture in the same area. Because terrestrial LiDAR systems usually have shorter ranges and much higher point density, those object surface data works well for the airborne LiDAR system as reference data. Three approaches are used for extracting conjugate features; pseudo-conjugate points by ICP, conjugate points/triangles by ICPatch, and conjugate planar patches by plane segmentation. And the real data test shows that existing bore-sighting parameters are improved after calibrating system using LiDAR raw measurement, which is confirmed by calculating the normal distances between reference surfaces and adjusted surfaces. For increasing the robustness and reliability of the LiDAR system calibration, strong surface match procedure should be also considered in the future.

REFERENCES

Baltsavias, E., 1999. Airborne laser scanning: existing systems and firms and other resources, ISPRS Journal of Photogrammetry and Remote Sensing, 54 (2-3): 164-198.

Bretar F., M. Pierrot-Deseilligny, and M. Roux, 2004. Solving the Strip Adjustment Problem of 3D Airborne Lidar Data., Proceedings of the IEEE IGARSS'04, 20-24 September, Anchorage, Alaska.

Crombaghs, M., E. De Min, and R. Bruegelmann, 2000. On the Adjustment of Overlapping Strips of Laser Altimeter Height Data. *International Archives of Photogrammetry and Remote Sensing*, 33(B3/1): 230-237.

Filin, S., 2003. Recovery of systematic biases in laser altimetry data using natural surfaces. *Photogrammetric Engineering and Remote Sensing*, 69(11):1235–1242.

Habib, Ayman, Rita W.T. Cheng, Eui-Myoung Kim, Edson A. Mitishita, Richard Frayne, and Janet L. Ronsky, 2006. Automatic Surface matching for the Registration of LiDAR Data and MR Imagery. *ETRI Journal*, Vol. 28, No. 2: 162-174.

Hanjin Information System & Telecommunication Co. Ltd, 2006. "Computing Determinant method for Calibrating Airbornelaser Surveying System (Patent Document)", <http://patent2.kipris.or.kr/patent/KP/KPD11010.jsp#Book10> (accessed 1 Sep. 2006)

Huising, E. J., and L. M. G. Pereira, 1998. Errors and Accuracy Estimates of Laser Data Acquired by various Laser Scanning Systems for Topographic Applications, *ISPRS Journal of Photogrammetry and Remote Sensing*, 53(5): 245-261.

Kilian, J., N. Haala, and M. Englich, 1996. Capture and evaluation of airborne laser scanner data. *International Archives of Photogrammetry and Remote Sensing*, 31(B3):383–388.

Maas, H. G., 2000. Least-Squares Matching with Airborne Laserscanning Data in a TIN Structure. *International Archives of Photogrammetry and Remote Sensing*, 33(B3/1): 548-555.

Schenk, T. 2001. Modeling and Analyzing Systematic Errors in Airborne Laser Scanners, Technical Report in Photogrammetry, No. 19, Ohio Sate University.

Skaloud, J. and D. Lichti, 2006. Rigorous Approach to Bore-Sight Self-Calibration in Airborne Laser Scanning. *ISPRS Journal of Photogrammetry and Remote Sensing*, 61: 47–59.

Zhang, Z., 1994. Iterative point matching for registration of free-form curves and surfaces, *International Journal of Computer Vision*, 13(2):119 – 152.

ACKNOWLEDGEMENT

The authors would like to thank the NSERC and the GEOIDE Network of Centers of Excellence of Canada (SII#43 and TDMASR37) for their partial financial support of this research.

